Journal of Applied Polymer Science

Taguchi-Based Analysis of Polyamide 6/Acrylonitrile–Butadiene Rubber/Nanoclay Nanocomposites: The Role of Processing Variables

Ali Ebrahimi Jahromi,[1] Ahmad Arefazar,[2] Omid Moini Jazani,[3] Morteza Ganjaee Sari,[4] Mohammad Reza Saeb,[5] Mohammad Salehi[1]

[1]Higher Education Department, Islamic Azad University, South Tehran Branch, Tehran, Iran
[2]Department of Polymer Engineering and Color Technology, Amirkabir University of Technology, Tehran, Iran
[3]Department of Chemical Engineering, College of Engineering, University of Isfahan, Isfahan, Iran
[4]Department of Nanomaterials and Nanocoatings, Institute for Color Science and Technology, Tehran, Iran
[5]Department of Resin and Additives, Institute for Color Science and Technology, Tehran, Iran
Correspondence to: A. Arefazar (E-mail: arefazar@aut.ac.ir)

ABSTRACT: Applying the Taguchi method of experimental design, we prepared various polyamide 6 (PA6)/acrylonitrile butadiene rubber (NBR)/nanoclay nanocomposites under different processing conditions by melt mixing in an internal mixer. The effects of the processing variables, including the rotor speed, chamber temperature, and mixing order on the morphology, that is, the rubber particle size and interlayer distance, and the mechanical properties, that is, the tensile modulus and impact strength, were then investigated. As demonstrated with the Taguchi approach, the lower temperature associated with higher rotor speeds improved the mechanical properties of the 90/5/5 PA6/NBR/nanoclay systems. However, it was revealed that the mixing order did not affect the mechanical properties for the assigned composition. Hence, the simultaneous mixing of all the ingredients is seemingly the simplest way of mixing to obtain the desired mechanical properties. These results were confirmed with transmission and scanning electron microscopy observations and X-ray diffraction measurements. Image analysis corresponding to the mean particle size of the NBR constituent was also performed. The optimum processing condition to achieve the appropriate mechanical properties is ultimately predicted by the Taguchi analysis and corresponded to a chamber temperature of 230°C and a screw speed of 80 rpm. Moreover, the simultaneous mixing of all of the ingredients was suggested for convenience. © 2013 Wiley Periodicals, Inc. J. Appl. Polym. Sci. 130: 820–828, 2013

KEYWORDS: Taguchi analysis; nanocomposites; PA6/NBR/Nanoclay; processing variables; interlayer distance

Received 27 November 2012; accepted 11 February 2013; published online 5 April 2013
DOI: 10.1002/app.39191

INTRODUCTION

Until now, extensive investigations have been carried out on the effective parameters that determine the dispersion of nanoclay particles and the particle size distribution in various nanocomposites prepared through melt mixing. Cho and Kamal[1] proposed a model to describe the exfoliated structure of nanoclay particles within nanocomposites. They demonstrated that the exfoliation of the nanoclay platelets depended on the shear rate, matrix viscosity, interlayer distance, and aspect ratio of the nanoplatelets. Also, increasing the shear rate enhanced the process of the layer exfoliation. In any case, the most important parameter that affected the ultimate morphology of the nanocomposites was the extent of interaction between the macromolecules and the nanoclay layers. For instance, the clay that showed an exfoliated morphology in nylon 6, because of inappropriate interactions, may have formed an intercalated structure in an ethylene vinyl alcohol copolymer matrix.[2] A comparative study proved that nanoclay can be dispersed more evenly in the nylon 6 matrix than in a nylon 66 one. The better interaction between the macromolecules of nylon 6 and nanoclay platelets is a reason for this phenomenon because, in an equal length of the polymer chain, nylon 6 possesses a greater number of polar groups than nylon 66.[3] Another study revealed that increasing the number of alkyl branches in the structure of the compatibilizer enhances the nanoclay dispersion throughout the linear low-density polyethylene matrix compared to that of the nylon 6 matrix.[4] Kamal et al. prepared high-density polyethylene/polyamide 66 (PA66)/clay nanocomposite in a twin-screw extruder and investigated the effect of the mixing duration on the exfoliation process.[5] With a prolonged mixing time, a more homogenized structure in the nanocomposite was observed. Albeit, it was shown that if a thermodynamically stable state is

reached, increasing the residence time in a constant shear rate does not affect the nanoclay dispersion.[6] Fornes and coworkers[7,8] studied the effect of the molecular weight of the polymer matrix on the exfoliation process. They found that the use of polymers with higher molecular weight improves the dispersion process. They reasoned this observation on account of the higher shear stress induced by the increase in the melt viscosity. It has been also revealed that the type of mixer has an impact on the dispersion and distribution of the nanoclay, as those that produce a higher shear rate cause a better dispersion and distribution of the nanoclay.[9,10]

In three-component nanocomposites, the location of the nanoclay as an effective parameter on the microstructure and, thus, the mechanical properties has recently been examined by several authors. In nanocomposites containing PA66, maleated poly[styrene-*b*-(ethylene-*co*-butylene)-*b*-styrene] triblock copolymer (SEBS-*g*-MA), and nanoclay, when the nanoclay lamellae were located in the PA66 matrix, the best balance between hardness and impact resistance was reached.[11,12] Similar trends were observed in poly(butylene terephthalate)/maleated ethylene vinyl acetate (EVA-*g*-MA)/clay and poly(ethylene terephthalate)/maleated ethylene–propylene diene (EPDM-*g*-MA)/clay nanocomposites.[13,14] Kelnar and coworkers[15,16] reported that when they added nanoclay to polyamide 6 (PA6)/ethylene–propylene rubber systems when the lamellae were situated around the ethylene–propylene rubber particles, the toughness increased. Furthermore, in a PP/EVA/nanoclay system, the location of the lamellae in the EVA phase significantly improved the impact resistance.[17]

In a previous articles on thermoplastic elastomers, the role of the mixing sequence in poly(ethylene terephthalate)/EPDM, EPDM-*g*-MA/organoclay ternary hybrid nanocomposites was evaluated in-depth.[14] Moreover, it was found that the state of dispersion in nanocomposites based on PA6/acrylonitrile–butadiene rubber (NBR) was somehow governed by the type of nanoclay, clay content, and mixing temperature.[18] A variety of nanocomposites were prepared, and their thermal and morphological characteristics were examined. The water-assisted approach has also been taken into consideration by others to prepare highly exfoliated polycarbonate/poly(methyl methacrylate)/clay nanocomposites.[19] As the number of variables and their variation range were large in case of the PA6/NBR/clay nanocomposites, the preparation of a thermoplastic elastomer representing an appropriate exfoliation of nanoclay within the thermoplastic matrix was seemingly a task of difficulty. We already studied the effects of the processing parameters on the ultimate properties of such systems employing an experimental design method.[20,21] Hence, the well-established Taguchi analysis was used in this study to corroborate the effects of the processing variables, namely, the rotor speed, temperature inside the internal mixer, and sequence of the mixing, on the microstructure and mechanical properties, that is, the modulus and impact resistance of 90/5/5 PA6/NBR/clay nanocomposites. On the basis of the knowledge developed in previous studies,[14,18] we paid attention to infer the alteration of the ultimate properties on the basis of the interlayer distance of the nanoclay and the rubbery-phase particle size.

THEORETICAL

Design of Experiments with the Taguchi Approach

The Taguchi approach provides an opportunity for the researchers to properly infer the variations in a specified process. This method was originally used in industrial environments to reduce the number of experiments needed for the interpretation of the effects of changing variables involved in processes. As proposed by Taguchi, this method is a statistical/mathematical means to organize the variation range of influential parameters toward one or more responding variables with orthogonal arrays. The main benefit of using the Taguchi approach, in addition to that of minimizing the number of experimental runs, is that the interpretation of the results is more precisely achievable in comparison with conventional approaches. In another words, this method allows the determination of the most significant factors among a series of changing variables. With orthogonal arrays, the full factorial design is transformed to a partial factorial design. Such transformation causes significant savings in both time and money. It is also possible to evaluate the precision and reliability of the data. Also, the interaction effects of each pair of changing variables, conventionally called *independent variables,* on the target factor can be understood. Therefore, the use of the orthogonal arrays technique results in a proper interpretation on the data and keeps the number of experimental runs sufficiently limited. One of the most appropriate orthogonal arrays in this method is a nine-experiment (L9) design. In this design, three independent variables are statistically changed at three different levels. In this study, the responding variables were optimized on the basis of the L9 experimental design.[22,23]

EXPERIMENTAL

Materials

NBR was purchased from Korea Kumho Petrochemical Co., Ltd., under the trade name KOSYN KNB 35L, Ulsan, Korea. This high oil- and chemically resistant copolymer was made from acrylonitrile (34%) and butadiene by cold emulsion polymerization. The Mooney viscosities of the raw and compounded NBRs (ML 1+4) at 100°C were 4s1 and 69, respectively, according to the supplier. The density of the noncompounded mixture was also reported to be 940 kg/m^3. PA6 was a commercial-grade polymer provided by Akulon F136-C1, DSM, Heerlen, the Netherlands. The density, melting point, and viscosity number of this constituent were 1.13 kg/m^3, 220°C, and 245 cm^3/g, respectively. The water and humidity absorption were also given in the data sheet as 9.5 and 2.5%, respectively. Unmodified montmorillonite (Cloisite 30B), with a bulk density of 228.3 kg/m^3 and a moisture content of 2%, was also purchased from Southern Clay Products Co. Before melt blending, the PA6 and nanoclay were placed in an oven at 80°C for 24 h to prevent moisture absorption.

Sample Preparation

As stated, to evaluate the impact of the independent parameters on the responding variables, a Taguchi L9 orthogonal array was used. The three independent variables chosen based on a literature review in this investigation were as follows: the chamber temperature, rotor speed, in rounds per minute (rpm), of the internal mixer, and mixing sequence. The whole ingredients,

Table I. Range of Variation in the Changing Parameters

Parameter	Symbol	Unit	Nominal levels
Chamber temperature	A	°C	230-240-250
Rotor speed	B	rpm	40-60-80
Blending sequence	C	—	M1-M2-M3

90 wt % PA6, 5 wt % NBR, and 5 wt % nanoclay, were transferred to a Brabender internal mixer (model W50 EHT), Duisburg, Germany, and after mixing, they were removed and placed on a sheet mold at 230°C to obtain sheets 3 mm in thickness by means of pressure. These sheets were used to prepare appropriate specimens for carrying out the experiments. Table I demonstrates the independent variables and their variation limits that optimized the processing conditions. In the M1 mixing procedure, the NBR, PA6, and nanoclay were simultaneously loaded into the mixer. In the M2 mixing method, at first, the PA6 and nanoclay blend was prepared, and then, NBR was added to this blend. In contrast, in the M3 mixing method, the PA6/NBR blend was first prepared, and then, the nanoclay was added in the next step. The results of the experimental design by the Taguchi method are given in Table II. The response variables were lamellar distance, rubber mean particle size (d), Young's modulus, and impact resistance. After we analyzed the results by the aim of the Taguchi method, the optimized processing condition are obtained.

Characterization

Rheological measurements were carried out by means of a stress-controlled rheometer (MCR300), Österreich, Austria equipped with parallel plates 25 mm in diameter at 230°C in the angular frequency range 0.1–100 rad/s. To assess the dispersion of nanoclay throughout the matrix, X-ray diffraction (XRD) at a small-angle test was used. A Philips XRD equipment X'Pert model, PANalytical, the Netherlands was used. The X-ray wavelength was 1.54056 Å, and the voltage of the accelerator was set to 40 kV. To observe the nanostructure of the nanoclay in the matrix, at first, the samples underwent microtomy at a temperature of −50°C with a Reichert OMU3, American Optical, USA ultramicrotome. The thickness of the cut samples was 80 nm. Then, to increase the contrast of NBR incised in the phases, the sample was stained with osmium tetroxide (OsO_4) vapor. In the end, a transmission electron microscope, a Philips model EM 208 S was used to observe the prepared samples with an accelerator voltage of 100 kV.

Table II. Processing Conditions for the Preparation of the PA6/NBR/Nanoclay Nanocomposites on the Basis of the Taguchi L9 Method

Sample code	A (°C)	B (rpm)	C (—)
S1	230	40	M1
S2	230	60	M2
S3	230	80	M3
S4	240	40	M2
S5	240	60	M3
S6	240	80	M1
S7	250	40	M3
S8	250	60	M1
S9	250	80	M2

Also, to evaluate the dispersion state of the rubber particles within the nanocomposites, the samples were broken into pieces in liquid nitrogen for 2 min. The fracture surfaces were then put in acetone for 24 h until the NBR particles were extracted. Finally, the prepared samples were coated by gold. A scanning electron microscope (Philips model XL30) was used to take images of the samples. When the micrographs were taken, the accelerator voltage was kept unchanged at 30 kV. Image analysis was then carried out to determine the effect of the processing conditions on d of NBR. At least 200 NBR particles in each image were taken into consideration to calculate the mean rubber particle size. ImageJ, developed by National Institutes of Health software was used to analyze the state of dispersion of the rubbery domains through scanning electron microscopy (SEM).

Tensile testing was performed with a Zwick/Roell model KAP-TC, UK according to ASTM D 638 at a rate of 20 mm/min. Izod impact testing was carried out with a Zwick 5102, UK according to ASTM D 256. The notched samples for this test were created with a Ceast 6991.

RESULTS AND DISCUSSION

Through a frequency-sweep rheological test, the values of the complex viscosity of the PA6 and NBR neat constituents and the 95/5 PA6/nanoclay composite were obtained at 230°C and are plotted in Figure 1. The viscosity of PA6 at low shear rates (≤1 rad/s) remained almost constant; this indicated Newtonian behavior until it reached a region exhibiting a pseudo-plastic shear thinning trend at higher rates of deformation. However, the NBR complex viscosity indicated power-law type behavior over the entire range of angular frequencies. It is worth mentioning that incorporation of nanoclay with PA6, that is, in the 95/5 PA6/nanoclay system, caused a viscosity upturn toward the neat NBR curve, wherein a power-law melt came into being.

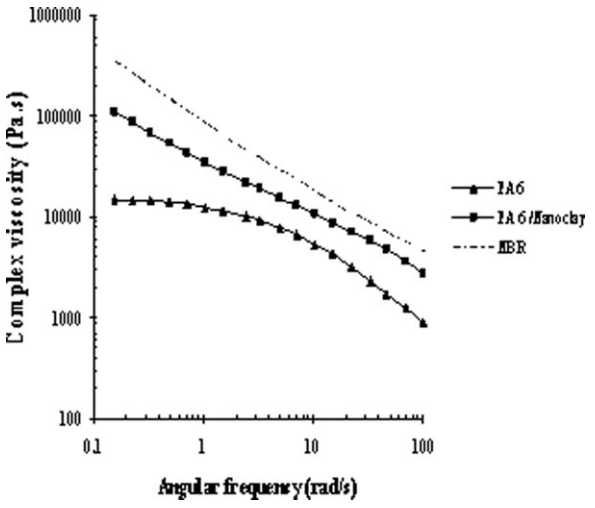

Figure 1. Complex viscosity as a function of the angular frequency for the neat NBR, PA6, and 95/5 mixture of PA6 and nanoclay at 230°C.

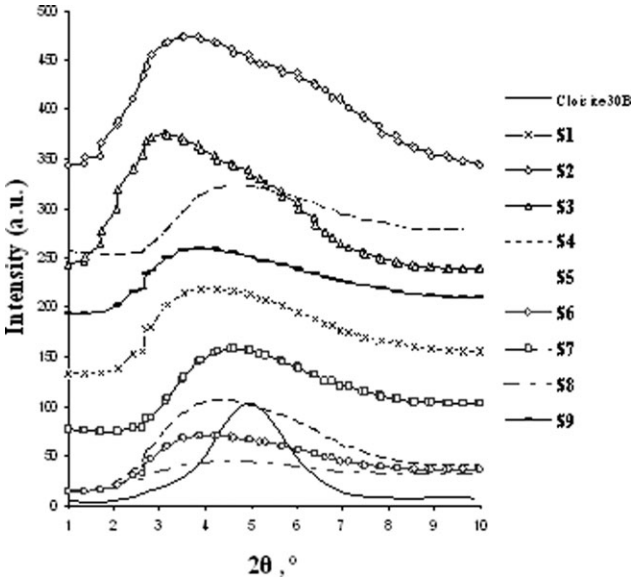

Figure 2. XRD patterns of the Cloisite 30B nanoclay and PA6/NBR/nanoclay nanocomposites.

This observation suggested a matching of the melt viscosities and mixing of the whole ingredients.

The effect of the processing conditions, including the chamber temperature, rotor speed, and mixing order on the state of dispersion of the nanoclay in these nanocomposites was analyzed by the use of XRD measurements. Figure 2 shows the XRD patterns for the pure nanoclay and the whole, prepared nanocomposite samples.

As it is clear, the distinctive maximum peak for pure nanoclay appeared at $2\theta = 4.85°$; this corresponded to a *d*-spacing of 18.5 Å. This peak was seen for all of the samples at lower angles ($2\theta < 4.85$), and this indicated that the distance between the layers of the nanoclay increased after the melt-mixing process. The calculated *d*-spacing values for Cloisite30B and nine other samples are reported in Table III.

Table III. Interlayer Distances (*d*-Spacings) of the Neat Nanoclay and PA6/NBR/Nanoclay Nanocomposites Prepared on the Basis of the Taguchi L9 Method

Sample code	2θ (°)	*d*-spacing (Å)
Cloisite 30 B	4.8	18.5
1S	3.58	22.82
S2	3.85	24.64
S3	3.17	27.82
S4	3.94	22.37
S5	4.12	21.42
S6	3.69	23.90
S7	4.61	19.16
S8	4.47	19.74
S9	4.06	21.81

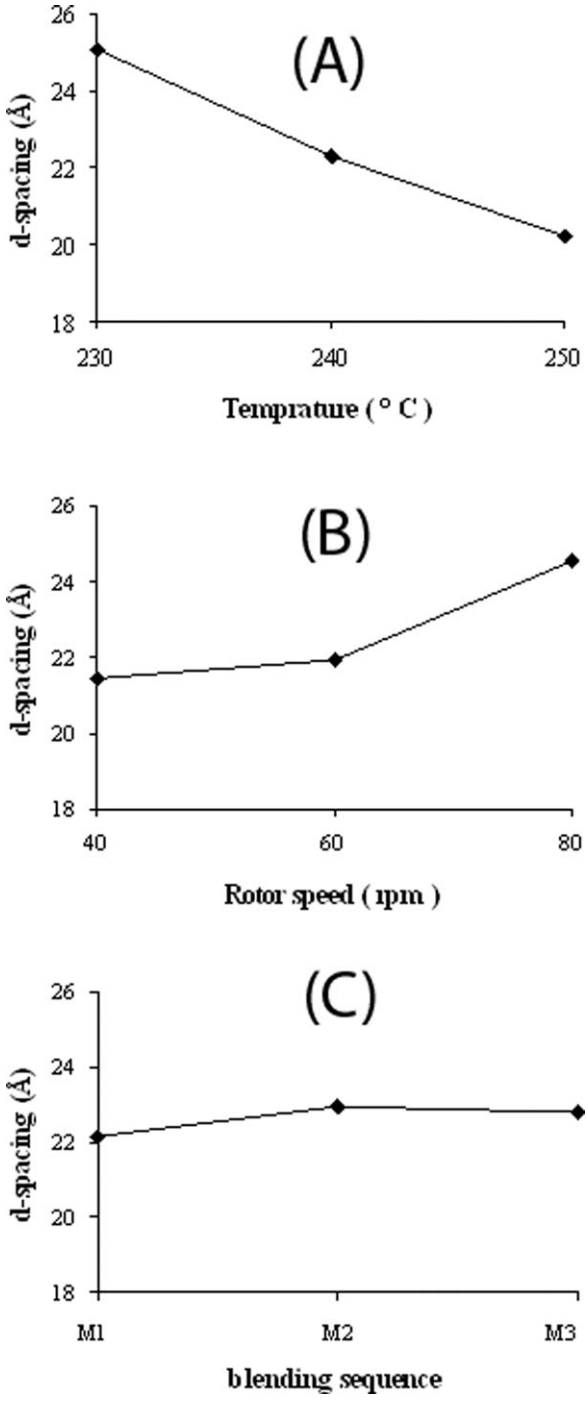

Figure 3. Mean effects of the (A) temperature, (B) rotor speed, and (C) order of mixing on the *d*-spacing of the nanoclay galleries in the 90/5/5 PA6/NBR/nanoclay nanocomposites.

The results suggest that an intercalated structure was formed and the nanoclay retained its ordered structure. As shown in Table III, the S3 sample containing 5% NBR and 5% nanoclay showed a diffraction peak at $2\theta = 3.17°$ related to a *d*-spacing of 27.82 Å; this was the maximum distance among all of the prepared samples. Such a significant increase could be attributed to better intercalation of the chains into the nanoclay layers for that sample. As the L9 orthogonal arrays randomized the

Applied Polymer SCIENCE

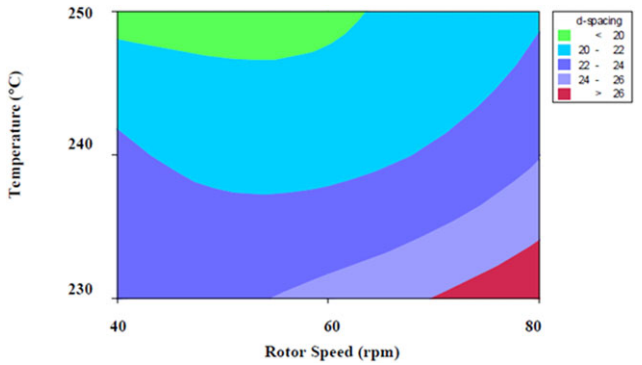

Figure 4. Contour plots of *d*-spacing (Å) indicating the interactive effects of the mixing temperature and intensity. [Color figure can be viewed in the online issue, which is available at www.wileyonlinelibrary.com.]

changing variables in a manner in which a conventional comparison was not explicitly possible, we concluded that the lower temperature associated with the higher rotor speed improved the mechanical properties, regardless of the mixing order. Further discussions should be made with the Taguchi approach, which corroborated the variation of responding variable with simultaneous changes in the processing parameters.

Figure 3 illustrates the curves that show the main effects of the chamber temperature, rotor speed, and mixing order on the distance between the layers of the nanoclay in the prepared nanocomposites according to the Taguchi analysis.

As observed in Figure 3(A), the *d*-spacing decreased with increasing chamber temperature. Such a decrease at higher temperatures may have been due to the decreased viscosity of PA6. Consequently, this fall in viscosity decreased the shear rate of the lamellae of the nanoclay. Also, the results show that the *d*-spacing steadily improved as the speed of the rotors in the mixing chamber increased [see Figure 3(B)]. This was also because of the increase in the shear tension on the lamellae. In fact, the shear rate applied across the mixing length caused the agglomerations to break and facilitated the diffusion of the polymer chains into the interlayer space of the lamellae.[24] In contrast to the aforementioned influences of the mixing temperature and intensity, the mixing order in these nanocomposites had no significant effect on the *d*-spacing [Figure 3(C)].

To deeply interpret the simultaneous effects of the changing parameters on the desired response, a contour plot representation in *xy* coordinate can be employed. In this plot, each colored area is indicative of a constant value of the responding variable. In Figure 4, the counter plots are given to demonstrate the simultaneous effects of the temperature and rotor speed, an interactive effect, on the *d*-spacing. As illustrated, at lower temperatures and higher degrees of mixing, the maximum *d*-spacing was achievable.

The XRD measurements revealed an intercalated structure of the nanoclay within the nanocomposites. However, by means of the transmission electron microscopy (TEM) technique, the extent of exfoliation and the localization of the nanoclay particles were uncovered. Figure 5 shows comparative TEM images for S3, S8, and S9. As mentioned previously, the NBR particles

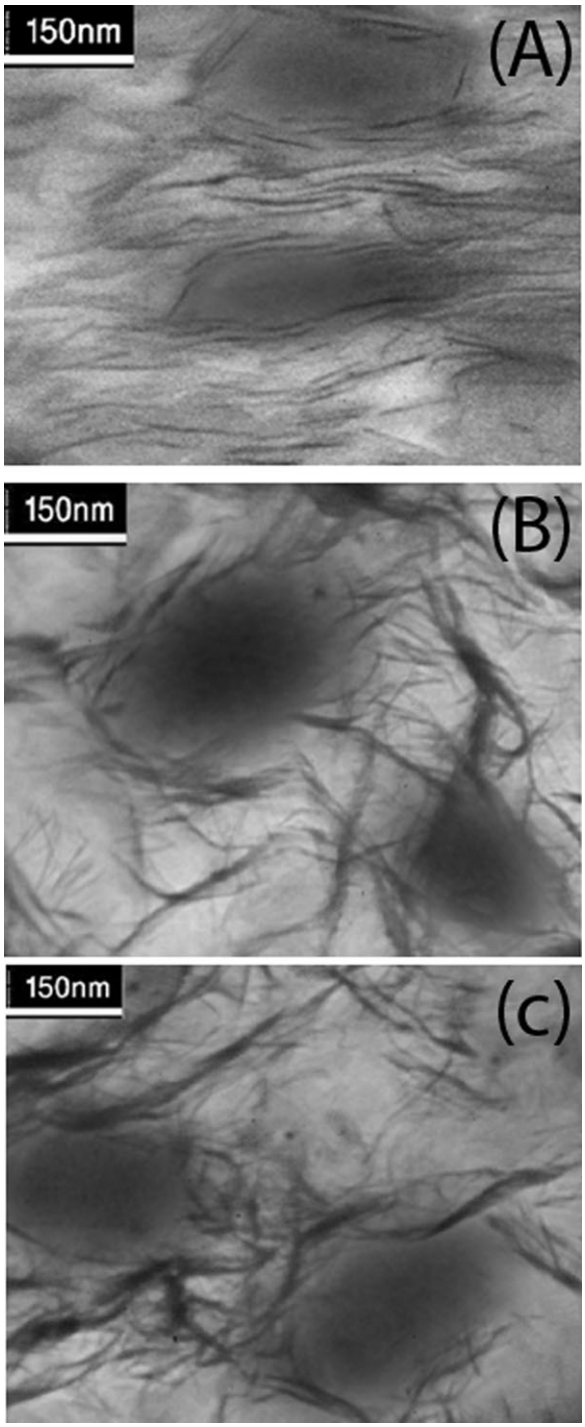

Figure 5. TEM images for the (A) S3, (B) S8, and (C) S9 90/5/5 PA6/NBR/nanoclay nanocomposites.

were stained by OsO_4 to increase contrast among the phases. The black lines in the images are the nanoclay particles.

In all of the samples, a combination of exfoliated and intercalated structures was distinguishable. As observed, S3 showed improved exfoliated and intercalated structures compared to S8 and S9. Agglomerations of the nanoclay layers were still detectable in S8 and S9. The higher polarity of PA6 compared to NBR

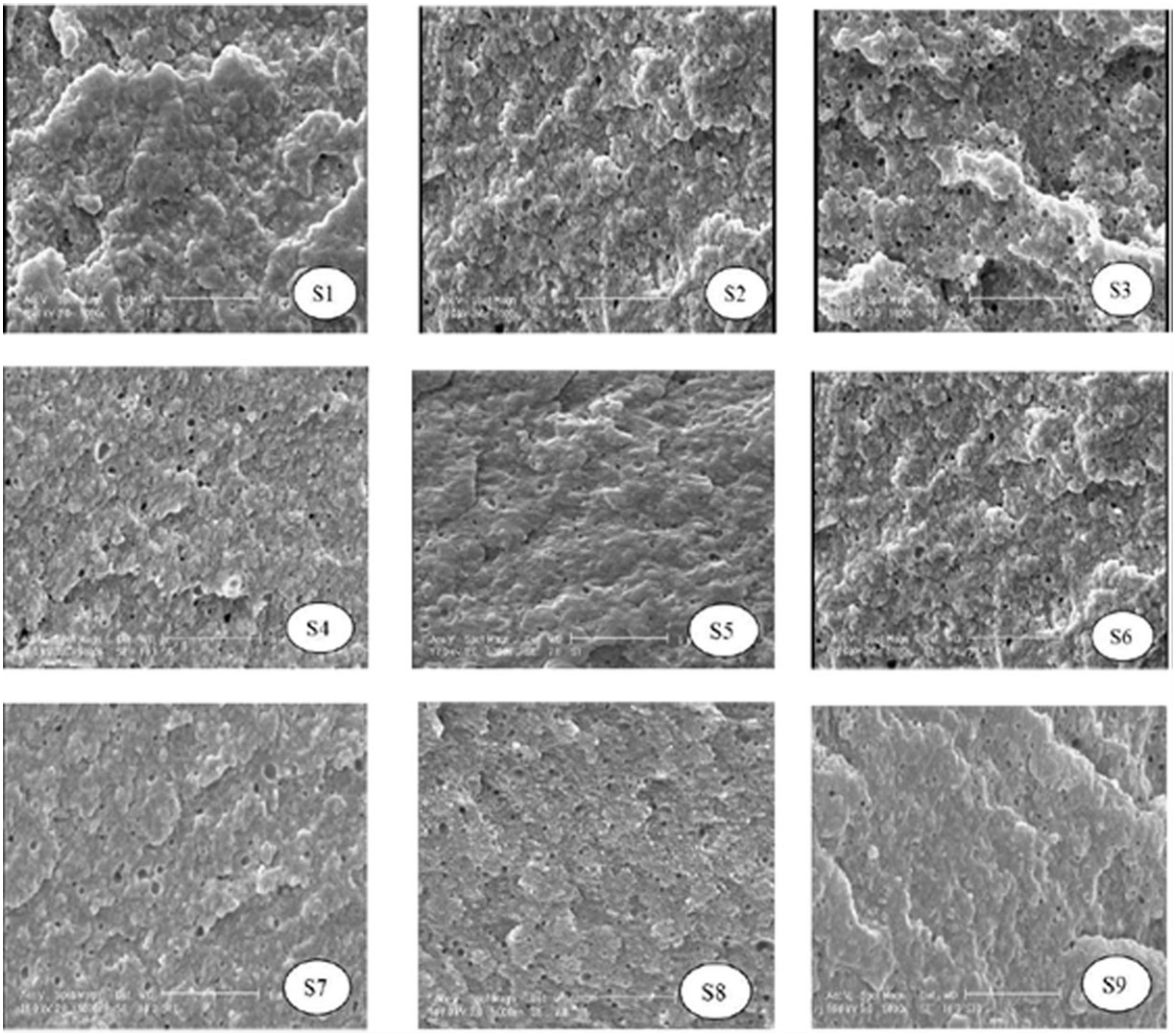

Figure 6. SEM micrographs for all of the 90/5/5 PA6/NBR/nanoclay nanocomposites corresponding to Table II.

caused the nanoclay to interact with the continuous phase, and that is why the major part of the nanoclay particles was in the polyamide phase. Also, because of the polar instinct of NBR, in all of the samples, the rubber particles were perfectly surrounded by the nanoclay layers. Although the images demonstrate that the nanoclay layers were not enveloped by the NBR phase, the TEM images entirely confirm the XRD measurements.

As discussed before, to investigate the distribution of rubber particles in the PA6 matrix, the rubber phase was selectively extracted with acetone. Figure 6 shows SEM images of these samples. The black holes in the images represent the rubber droplets extracted by the solvent. As clearly shown in Figure 6, the distribution of the rubber particles in S3 was much better, and its fracture surface seemed to be rougher compared to the other samples. The mean NBR particle size within the nanocomposites was calculated with an image analyzer, where at least 2000 particles for each sample were detected.

With the L9 Taguchi analysis, the role of the temperature, mixing intensity, and blending sequence on d of the NBR rubbery domains were obtained, as shown in Figure 7.

The quantitative comparison of d of the rubbery domains is also reported in Table III. Accordingly, the d values of all of the samples were in the range 164–230 nm. The minimum value corresponded to the S3 sample, in which the rubber particles were smaller and also the fracture surface was rougher; this indicated that this sample had the most acceptable dispersion among all of the prepared nanocomposites. The rubber particles showed a smaller size when the temperature was low and the mixing intensity (rotor speed) was relatively high. These observations were in good agreement with the XRD results and TEM images at low temperatures and high rotor speeds; this indicated improved intercalation and exfoliation because of the reduction of the rubber particle size. Once again, in the range of changing variables, the mixing order did not have a significant effect on the rubber particle size [Figure 7(C)].

Figure 8 shows contour diagrams, which provide a better understanding of the effect of the parameters, that is, the temperature and rotor speed, on d.

As we observed, we could obtain the best criterion for obtaining the minimum particle size of NBR in different ways while

Applied Polymer SCIENCE

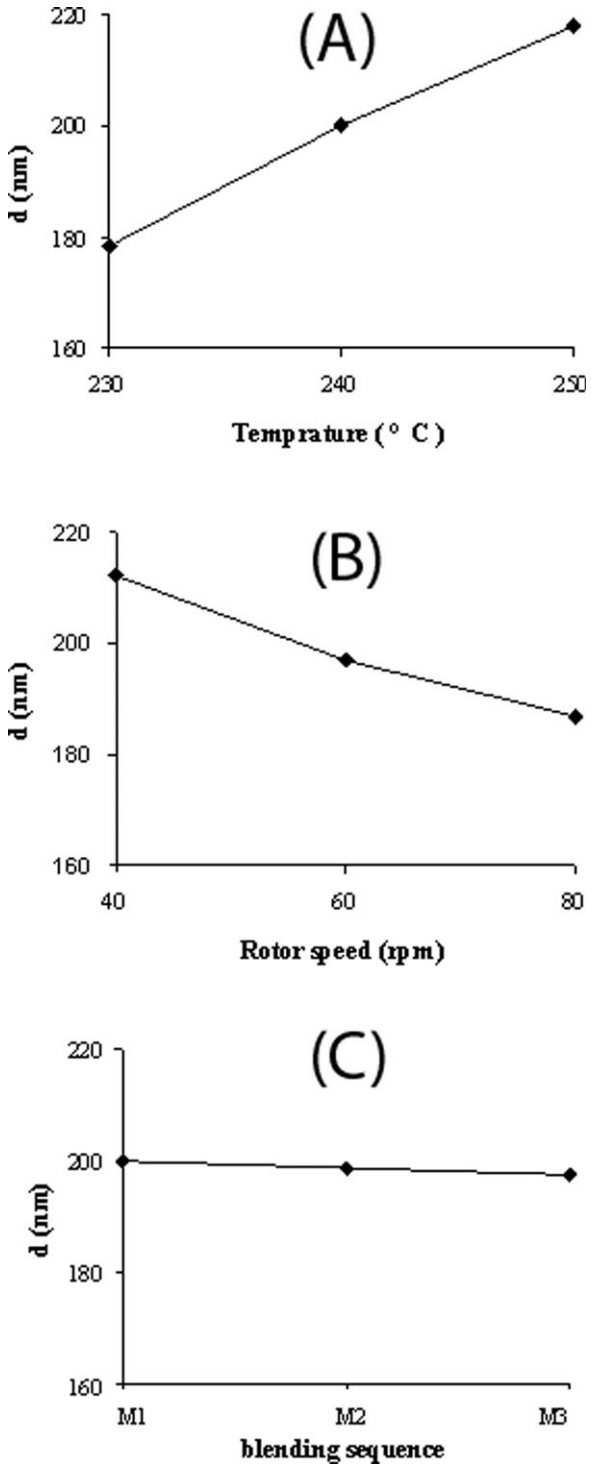

Figure 7. Mean effects of the (A) temperature, (B) rotor speed, and (C) order of mixing on *d* of the NBR rubbery constituent.

altering the mixing temperature and intensity simultaneously. Therefore, from an economic point of view, it would be better to choose lower temperatures and moderate rotor speeds, which results in lower phase domains. However, to access the best situation corresponding to particles with diameters lower than 170 nm, the Taguchi-based analysis suggested the use of the highest

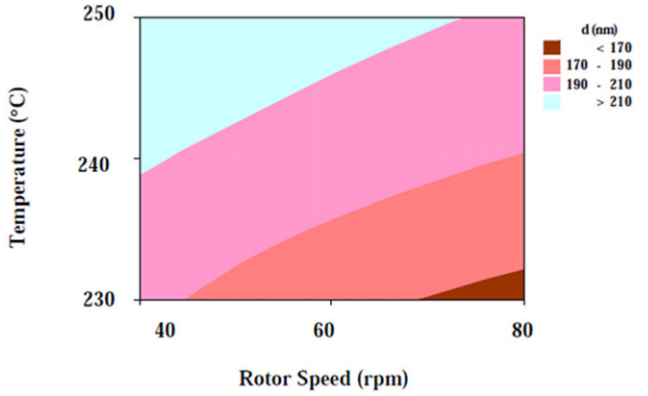

Figure 8. Contour plots of *d* of the NBR domains (nm) indicating the interactive effects of the mixing temperature and intensity. [Color figure can be viewed in the online issue, which is available at www.wileyonlinelibrary.com.]

rotor speed of 80 rpm. The mechanical properties, including the tensile modulus and impact resistance, of the samples are given in Table IV.

Normally, the state of dispersion in nanocomposites is greatly governed by the mixing procedure. A glance at Table IV reveals that the interpretation of mechanical properties on the basis of the NBR *d* seems a task of difficulty because of the random nature of the fluctuations of changing variables (see Table III). Figure 9 shows the effects of the chamber temperature, rotor speed, and mixing order on the tensile modulus of the prepared nanocomposites.

The only parameter that could increase the modulus of the samples containing 5% nanoclay was the degree of intercalation and exfoliation. As shown in Figure 9, the modulus increased when temperature went down and the mixing intensity increased. Such an increase in the modulus was related to the increase in intercalation and exfoliation structure, as shown in the XRD and TEM results.

Table IV. Interpretation of the Tensile Modulus and Impact Strength Values of the Prepared Nanocomposites with the *d* Values of the NBR Rubbery Constituent

Sample code	Tensile modulus (MPa)	Impact resistance (J/m)	*d* (nm)
PA6	2647 ± 91	1.85 ± 0.15	—
S1	3346 ± 13	2.44 ± 0.33	195
S2	3389 ± 15	2.55 ± 0.41	176
S3	3410 ± 62	2.66 ± 0.37	164
S4	3310 ± 81	2.35 ± 0.21	212
S5	3356 ± 12	2.43 ± 0.33	199
S6	3361 ± 11	2.46 ± 0.28	189
S7	3235 ± 10	2.17 ± 0.19	230
S8	3266 ± 12	2.25 ± 0.21	216
S9	3311 ± 11	2.30 ± 0.17	208

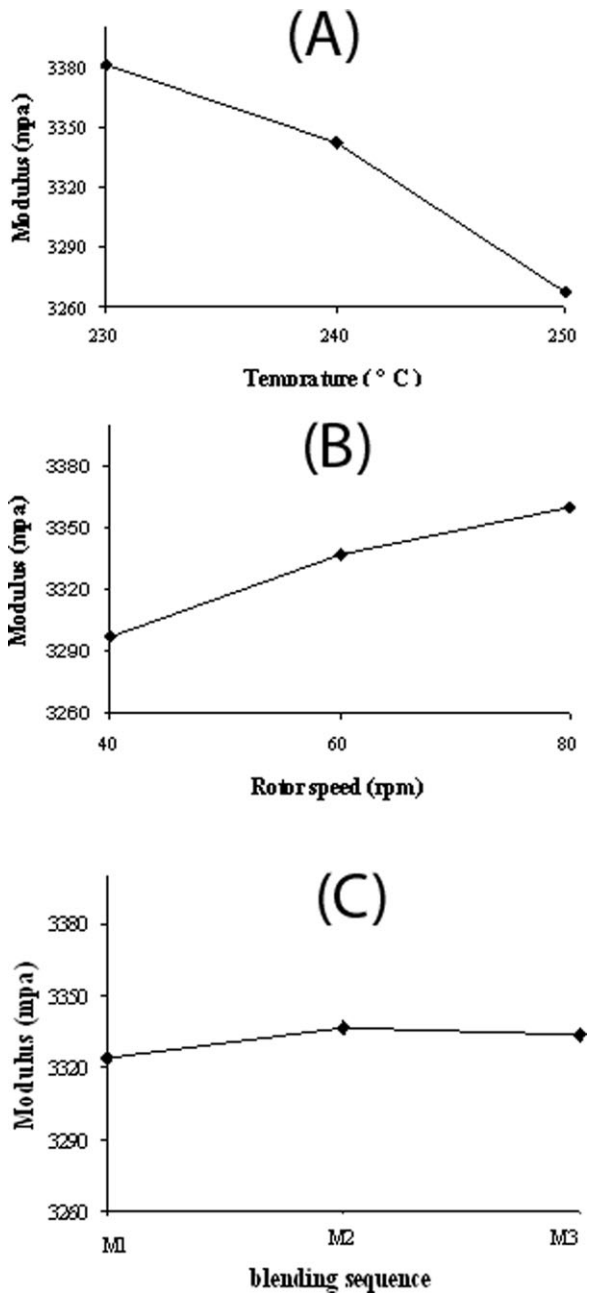

Figure 9. Mean effects of the (A) temperature, (B) rotor speed, and (C) order of mixing on the tensile modulus of the 90/5/5 PA6/NBR/nanoclay nanocomposites.

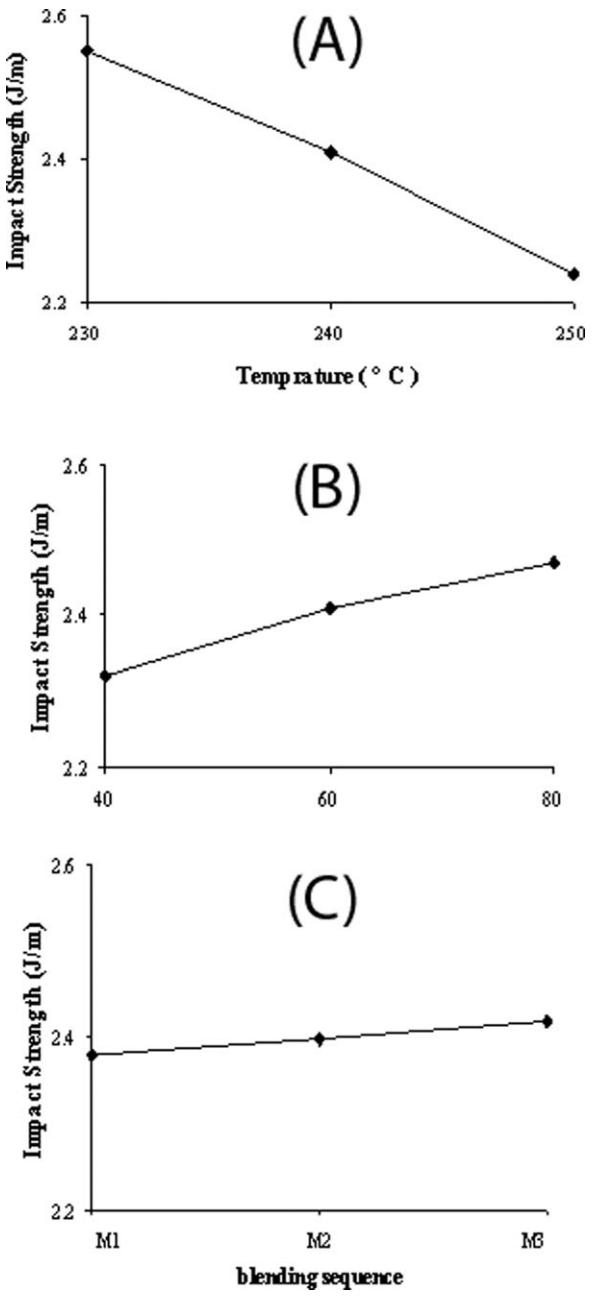

Figure 10. Mean effects of the (A) temperature, (B) rotor speed, and (C) order of mixing on the impact strength of the 90/5/5 PA6/NBR/nanoclay nanocomposites.

Figure 10 demonstrates the effects of the chamber temperature, rotor speed, and blending sequence on the impact resistance.

Comparatively, a decrease in the rubber particle size caused improved impact resistance in the nanocomposites. Also, as shown in Figure 10(A,B), the impact strength decreased with decreasing temperature and increasing rotor speed; this was in good agreement with SEM outcomes. As shown in Table IV, S3 showed the best balance between the tensile modulus and the impact strength. In this sample, the modulus increased 22% compared to pure PA6, and also, an increase of 43% in the impact resistance occurred. As the mixing order did not affect the morphology and mechanical properties of the nanocomposites, the simultaneous mixing of ingredients (M1) could be considered the simplest method of mixing. Contour plots of the impact data as a function of the mixing temperature and rotor speed given in Figure 11 revealed a similar trend previously seen for the mean NBR particle size (Figure 8) and interlayer distance (Figure 4). Ultimately, we found that the best sample representing the highest value of impact strength was prepared at 230°C and 80 rpm. This improvement in the mechanical properties was attributed to the better dispersion of the NBR rubbery domains with the minimum size associated with a

Applied Polymer SCIENCE

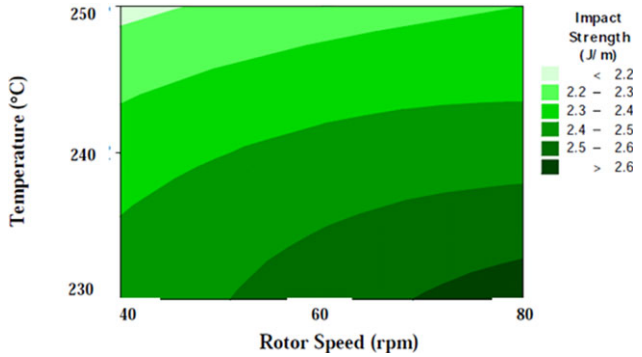

Figure 11. Contour plots of the impact strength (J/m) indicating the interactive effects of the mixing temperature and intensity. [Color figure can be viewed in the online issue, which is available at www.wileyonlinelibrary.com.]

reasonably intercalated and exfoliated morphology under the assigned processing conditions.

CONCLUSIONS

A variety of 90/5/5 nanocomposites of PA6/NBR/nanoclay were prepared by melt mixing in an internal mixer in accordance with an L9 Taguchi method of experimental design. Among the different processing conditions considered by the researchers, the rotor speed, chamber temperature, and mixing order were chosen to infer the alteration of the morphological and mechanical characteristics on the basis of the Taguchi approach. Different tools, XRD, SEM, and TEM, were then used to evaluate the state of dispersion of the nanoclay and NBR rubbery domains throughout the nanocomposites. To quantitatively study the role of the rubber particle size on the mechanical properties, image analysis was performed on the SEM micrographs. The nanoclay interlayer distance was also taken into consideration with XRD measurements. With the mean and interactive plots provided by the Taguchi design, we found that lowering the mixing temperature and increasing the mixing intensity (rotor speed) led to enhanced mechanical properties. Also, it was revealed that the mixing order did affect the mechanical properties, as proven by TEM and SEM observations and XRD measurements. Regardless of the blending sequence, in the range of processing variables, the best sample was obtained when the chamber temperature and rotor speed were set to 230°C and 80 rpm, respectively.

REFERENCES

1. Cho, Y.; Kamal, M. R. *Polym. Eng. Sci.* **2004**, *44*, 1187.
2. Artzi, N.; Narkis, M.; Siegmann, A. J. *Polym. Sci. Part B: Polym. Phys.* **2005**, *43*, 1931.
3. Chavarria, F.; Paul, D. R. *Polymer* **2004**, *45*, 8501.
4. Hotta, S.; Paul, D. R. *Polymer* **2004**, *45*, 7639.
5. Kamal, M. R. Presented at International Symposium on Polymer Nanocomposites Science and Technology, Boucherville, Quebec, Canada, October **2003**.
6. Yang, K.; Ozisik, R. *Polymer* **2006**, *47*, 2849.
7. Fornes, T. D.; Yoon, P. J.; Keskkula, H.; Paul, D. R. *Polymer* **2001**, *42*, 9929.
8. Fornes, T. D.; Yoon, P. J.; Hunter, D. L.; Keskkula, H.; Paul, D. R. *Polymer* **2002**, *43*, 5915.
9. Ko, M. B.; Lim, S.; Kim, J.; Choe, C. R.; Lee, M. S.; Ha, M. G. *Korea Polym. J.* **1999**, *7*, 310.
10. Yoon, J. T.; Jo, W. H.; Lee, M. S.; Ko, M. B. *Polymer* **2001**, *42*, 329.
11. Dasari, A.; Yu, Z. Z.; Mai, Y. W. *Polymer* **2005**, *46*, 5986.
12. Dasari, A.; Yu, Z. Z.; Yang, M. S.; Zhang, Q. X.; Xie, X. L.; Mai, Y. W. *Compos. Sci. Technol.* **2006**, *66*, 3097.
13. Li, X. C.; Park, H. M.; Lee, J. O.; Ha, C. S. *Polym. Eng. Sci.* **2002**, *42*, 2156.
14. Khatibi, M. A.; Arefazar, A.; Esfandeh, M. *e-Polymers* **2008**, no. 164.
15. Kelnar, I.; Kotek, J.; Kapralkova, L.; Hromadkova, J.; Kratochvil, J. J. *Appl. Polym. Sci.* **2006**, *100*, 1571.
16. Kelnar, I.; Khunova, V.; Kotek, J.; Kapralkova, L. *Polymer* **2007**, *48*, 5332.
17. Martins, C. G.; Larocca, N. M.; Paul, D. R.; Pessan, L. A. *Polymer* **2009**, *50*, 1743.
18. Mahallati, P.; Arefazar, A.; Naderi, G. Iranian J. *Chem. Eng.* **2011**, *8*, 56.
19. Dhibar, S.; Kar, P.; Khatua, B. B. *J. Appl. Polym. Sci.* **2012**, *125*, 601.
20. Moini Jazani, O.; Arefazar, A.; Saeb, M. R.; Ghaemi, A. J. *Appl. Polym. Sci.* **2010**, *116*, 2312.
21. Moini Jazani, O.; Arefazar, A.; Jafari, S. H.; Saeb, M. R. *J. Polym. Eng.* **2011**, *31*, 237.
22. Montgomery, D. C. Design and Analysis of Experiments, 6th ed.; Wiley: New York, **2005**; p 464.
23. Roy, R. K. Design of Experiments Using Taguchi Approach; Wiley: New York, **2001**; p 8.
24. Kim, S. W.; Ho Jo, W.; Lee, M. S.; Ko, M. B.; Jho, J. Y. *Polym. J.* **2002**, *34*, 103.